Molecules and Cells

Hepatitis C Virus Nonstructural Protein 5A Interacts with Immunomodulatory Kinase IKKε to Negatively Regulate Innate Antiviral Immunity

Sang-Min Kang[1,2], Ji-Young Park[2,3], Hee-Jeong Han[1], Byeong-Min Song[1], Dongseob Tark[1], Byeong-Sun Choi[2,*], and Soon B. Hwang[4,5,*]

[1]Laboratory for Infectious Disease Prevention, Korea Zoonosis Research Institute, Jeonbuk National University, Iksan 54531, Korea, [2]Division of Chronic Viral Disease, Center for Emerging Virus Research, National Institute of Infectious Diseases, National Institute of Health, Korea Disease Control and Prevention Agency, Cheongju 28159, Korea,[3]Department of Veterinary Public Health, College of Veterinary Medicine, Jeonbuk National University, Iksan 54596, Korea, [4]Laboratory of RNA Viral Diseases, Korea Zoonosis Research Institute, Jeonbuk National University, Iksan 54531, Korea, [5]Ilsong Institute of Life Science, Hallym University, Seoul 07247, Korea
*Correspondence: sbhwang@jbnu.ac.kr (SBH); byeongsun@korea.kr (BSC)
https://doi.org/10.14348/molcells.2022.0018
www.molcells.org

Hepatitis C virus (HCV) infection can lead to chronic hepatitis, liver cirrhosis, and hepatocellular carcinoma. HCV employs diverse strategies to evade host antiviral innate immune responses to mediate a persistent infection. In the present study, we show that nonstructural protein 5A (NS5A) interacts with an NF-κB inhibitor immunomodulatory kinase, IKKε, and subsequently downregulats beta interferon (IFN-β) promoter activity. We further demonstrate that NS5A inhibits DDX3-mediated IKKε and interferon regulatory factor 3 (IRF3) phosphorylation. We also note that hyperphosphorylation of NS5A mediats protein interplay between NS5A and IKKε, thereby contributing to NS5A-mediated modulation of IFN-β signaling. Lastly, NS5A inhibits IKKε-dependent p65 phosphorylation and NF-κB activation. Based on these findings, we propose NS5A as a novel regulator of IFN signaling events, specifically by inhibiting IKKε downstream signaling cascades through its interaction with IKKε. Taken together, these data suggest an additional mechanistic means by which HCV modulates host antiviral innate immune responses to promote persistent viral infection.

Keywords: DDX3, hepatitis C virus, IFN-β, IKKε, IRF3, NS5A

INTRODUCTION

Hepatitis C virus (HCV) is a major causative agent of chronic liver disease, including liver cirrhosis and hepatocellular carcinoma (Hoofnagle, 2002; Saito et al., 1990). Approximately 80% of individuals infected with HCV become chronic infection. HCV is an enveloped virus with a positive-sense, single-stranded RNA genome ans belongs to the genus *Hepacivirus* in the family *Flaviviridae*. The HCV genome is approximately 9.6 kb in length and encodes a large polyprotein precursor of ~3,000 amino acids, which is processed into 3 structural (core, E1, and E2) and 7 nonstructural (NS) proteins (p7 and NS2 to NS5B) (Lindenbach and Rice, 2005; Reed and Rice, 2000). Both structural and NS proteins of HCV interact with cellular proteins to regulate host cellular signaling transduction pathways, thereby facilitating viral persistence (Li et al., 2009; 2011; Matsumoto et al., 1996; Morikawa et al., 2011; Ray and Ray, 2001; Reyes, 2002).

Received 2 February, 2022; revised 23 May, 2022; accepted 23 May, 2022; published online 22 August, 2022

eISSN: 0219-1032

The host antiviral response is triggered by the detection of viral pathogen-associated molecular pattern (PAMP) (Jensen and Thomsen, 2012; Kawai and Akira, 2006). Retinoic acid-inducible gene-I (RIG-I) and Toll-like receptor 3 (TLR3) are major cellular receptors that recognize viral PAMP (Kawai and Akira, 2008; Saito et al., 2008; Yu and Levine, 2011). RIG-I and MDA5 detect a variety of viruses and signal the production of interferon (IFN) and induction of antiviral responses. HCV infection stimulates host innate immune responses after host sensing of viral RNA. Upon HCV infection, RIG-I is activated by 5′ppp-RNA and poly-U/UC in the 3′UTR region of the HCV genome. The question of whether HCV RNA is sensed by the MDA5 is still controversial. MDA5 is also activated by double-stranded RNA replicative intermediates produced during viral infection. Both RIG-I and MDA5 bind to viral RNA through caspase activation recruitment domain adaptor (CARD) domains and activate mitochondrial antiviral signaling protein (MAVS) (Seth et al., 2005). MAVS recruits TRAFs (TNF [tumor necrosis factor] receptor-associated factors), which are required for TANK-binding kinase 1 (TBK1) and IKK complex activation. These kinases activate IFN-regulatory factor 3 (IRF3) and nuclear factor-kappa-B (NF-κB) (Fitzgerald et al., 2003; Sharma et al., 2003). Phosphorylated IRF3 dimerizes and translocates to the nucleus, where it activates the promoters of IFNs, cytokines, and IFN-stimulated genes (ISGs) (Brownell et al., 2014; Kanda et al., 2007; Kawai and Akira, 2006; Lau et al., 2008; Lin et al., 1998; Metz et al, 2013). Type I IFN-stimulated genes are not activated in the absence of IKKε since ISGF3 does not bind to the promoter elements of ISGs (Lin et al., 1998; Ng et al., 2011; Tenoever et al., 2007). IKKε is linked to IFN-induced IFIT2 expression and the phosphorylation of STAT1, which occurs independently of IRF3 in West Nile virus infection (Perwitasari et al., 2011). Furthermore, IKKε controls constitutive, cancer cell-associated NF-κB activity via the regulation of Ser-536 p65/RelA phosphorylation (Adli and Baldwin, 2006).

A growing body of evidence indicates that DEAD box helicase 3 (DDX3) directly interacts with IKKε to enhance the induction of type I IFN (Gu et al., 2013; Schroder et al., 2008). The DDX3 C-terminal region directly binds to MAVS (also known as IPS-1, VISA, and CARDIF) CARD domain and regulates MAVS-mediated IFN-β promoter activation (Kawai et al., 2005; Oshiumi et al., 2010). Silencing of DDX3 impairs IKKε-induced IRF3 phosphorylation and IFN-β production. Many viruses have evolved to evade host immune response by targeting DDX3. For example, vaccinia virus K7 protein inhibits IFN-β promoter induction by binding to the N-terminal tail region of DDX3 (Schroder et al., 2008). Hepatitis B virus polymerase counteracts the host innate immune response by interacting with DDX3 to disrupt its interaction with IKKε (Yu et al., 2010).

HCV evades host antiviral innate immune responses to mediate persistent infection. However, the mechanisms employed by HCV to evade IFN-mediated antiviral responses are not completely understood. HCV has evolved multiple strategies to attenuate IFN-mediated innate immune response. HCV NS3/4A protease cleaves MAVS from mitochondria and TIR domain-containing adaptor-inducing interferon-β (TRIF) adaptor protein to shut down the TLR3-mediated signaling and type I IFN production (Ferreon et al., 2005; Li et al., 2005a; 2005b). Moreover, NS5A protein interacts with IFN-α-inducible double-stranded RNA-activated protein kinase (PKR) via its ISDR (IFN sensitivity-determining region) to regulate IFN-induced antiviral responses by activating eIF-2α and STAT1 (Gale et al., 1998; Noguchi et al., 2001; Wong et al., 1997). It has been previously reported that NS5A inhibits ISG expression by disrupting STAT1 phosphorylation and increasing IL-8 production (Lan et al., 2007; Polyak et al., 2001).

Since NS5A interacts with multiple cellular signaling transducers and exerts a wide range of effects on innate immune responses, we specifically explored the possible involvement of HCV NS5A in type I IFN-induced antiviral immunity. In the present study, we demonstrate that NS5A interacts with IKKε and inhibits IFN-β promoter activity. NS5A specifically inhibits IKKε-mediated IFN-β production through inhibiting DDX3-mediated IKKε phosphorylation. Importantly, hyperphosphorylation of NS5A is required for protein interplay with IKKε, thereby contributing to its significant role in the IFN-β signaling pathway. These data suggest that HCV exploits signal transduction components of host cells to maintain persistent infection.

MATERIALS AND METHODS

Plasmids and DNA transfection

Myc-tagged NS5A and GFP-tagged NS5A were described previously (Nguyen et al., 2020). Substitutions of serine to alanine at 2194, 2197, 2201, and 2204 hyperphosphorylation sites in NS5A were performed using a QuikChange® II XL Site-Directed Mutagenesis Kit (Stratagene, USA) according to the manufacturer's instructions. IFN-β-luc and ISRE-luc plasmids were provided by Dr. S. Goodbourn (St George's, University of London, UK). Flag-tagged IKKε wild-type, K38A, S172A, and TBK1 plasmids were provided by Dr. Kate Fitzgerald (University of Massachusetts, USA). Flag-tagged IKKε mutants (1-383, 1-299, 384-717, and 300-717) were generated by polymerase chain reaction (PCR) amplification of the relevant sequences from Flag-tagged wild-type IKKε and inserted into pCMV10-3x-FLAG (Sigma-Aldrich, USA). Myc-tagged and His-tagged DDX3 plasmids were provided by Dr. Andrew G. Bowie (Trinity College Dublin, Ireland). pEF-BOS-Flag-RIG-I, pEF-BOS-Flag-MDA5, and pEF-BOS-Flag-MAVS were provided by Dr. Takashi Fujita (Kyoto University, Japan). Full-length IRF3 was amplified by PCR using cDNA prepared from HEK293T cells and was subcloned into the pcDNA3.1/Myc-His vector (Invitrogen, USA). All DNA transfections were performed using a polyethyleneimine reagent (Sigma-Aldrich) as we described previously (Nguyen et al., 2020).

Cell culture

All cell lines were grown in Dulbecco's modified Eagle's medium (DMEM) containing 4,500 mg/L D-glucose, L-glutamine, and 110 mg/L sodium pyruvate (Thermo Fisher Scientific, USA) supplemented with 10% fetal bovine serum, 100 U/ml penicillin, and 100 mg/mL streptomycin. Huh7.5 cells were grown in DMEM supplemented with 10% fetal bovine serum (FBS), 1% MEM nonessential amino acids solution, 100 U/

mL penicillin, and 100 mg/ml streptomycin. Primary human hepatocytes (ScienCell Research Laboratories, USA) were grown in hepatocyte medium with 5% FBS, 100× hepatocyte growth supplement, and 1×10^7 units/L penicillin/10 g/L streptomycin in a poly-l-lysine-coated culture vessel.

Luciferase reporter assay

Luciferase and β-galactosidase assays were performed using either IFN-β-luciferase reporter plasmid or NF-κB-luciferase reporter plasmid and β-galactosidase plasmid as described previously (Nguyen et al., 2020). Huh7, Huh7.5, HepG2 cells were transfected with the reporter plasmid and β-galactosidase. At 12 h after transfection, cells were either mock-infected or infected with 100 HAU/ml of Sendai virus (SeV), or cells were treated with 500 ng/ml of poly I:C (InvivoGen, USA) for 24, 48, and 72 h. Luciferase reporter assays were performed according to the manufacturer's instructions (Promega, USA). SeV was provided by Dr. Byung-Yoon Ahn (Korea University, Korea).

RNA interference

siRNAs targeting two different regions of DDX3 (#1: 5′-UUC AAC AAG AAG AUC CAA CAA AUC C-3′; #2: 5′-GGG AGA AAU UAU CAU GGG AAA CAU U-3′) and the universal negative control siRNA were purchased from GenePharma (China). siRNA transfection was performed using a Lipofectamine RNAiMax reagent (Invitrogen) according to the manufacturer's instruction.

Quantification of RNA

Total RNA was extracted by using TRIZOL (Invitrogen) according to the manufacture's instructions. Reverse transcription to cDNA synthesis was performed using CellScript cDNA master mix (CellSafe, Korea) with 200 ng amount of RNA. Quantitative real-time PCR (qRT-PCR) was performed using iQ SYBR Green Supermix (Bio-Rad, USA) and QuantStudio 3 (Thermo Fisher Scientific) with the following primers: sense, 5′-CTT GGA TTC CTA CAA AGA AGC AGC-3′ and antisense, 5′-TCC TCC TTC TGG AAC TGC TGC A-3′ for IFN-β; sense, 5′-TGA CAG CAG TCG GTT GGA GCG-3′ and antisense, 5′-GAC TTC CTG TAA CAA CGC ATC TCA TA-3′ for actin.

ELISA

IFN-β was collected from cell culture supernatant and quantified with enzyme-linked immunosorbent assay (ELISA) using Human IFN-beta Quantikine ELISA Kit (R&D Systems, USA). ELISA was performed according to the manufacturer's instructions with triplicated experiments.

Immunoblot assay

Cells were washed twice in cold phosphate-buffered saline (PBS) and lysed in radioimmunoprecipitation assay (RIPA) buffer (25 mM Tris-HCl [pH 7.6], 150 mM sodium chloride [NaCl], 1% Nonidet P-40 [NP-40], 1% sodium deoxycholate, and 0.1% sodium dodecyl sulfate, protease inhibitor cocktail, and phosphatase inhibitor cocktail) for 15 min on ice. The samples were centrifuged at 15,000 rpm for 10 min at 4°C. The supernatant was collected and protein concentration was determined by the Bradford assay kit (Bio-Rad). Equal amounts of proteins were subjected to SDS-PAGE and electrotransferred to a nitrocellulose membrane. The membrane was blocked in TBS (Tris-buffered saline)-Tween (20 mM Tris-HCl [pH 7.5], 150 mM NaCl, and 0.05% Tween 20) containing 5% nonfat dry milk for 1 h and then incubated overnight at 4°C. The membrane was further incubated with following primary antibodies: α-IKKε, α-phospho-IKKε (Ser172), α-IRF3, α-phospho-IRF3 (Ser396), α-RIG-I, α-TBK1, α-MDA5, α-p65, and α-phospho-p65 (Ser536) from Cell Signaling Technology (USA); α-MAVS and α-DDX3 from Bethyl Laboratories (USA); α-LGP2 and α-GFP from Santa Cruz Biotechnology (USA); α-FLAG (M2) and α-β-actin from Sigma-Aldrich; α-c-Myc mouse monoclonal and α-6×-His-tag from Abcam (USA). Rabbit α-NS5A antibody was kindly provided by Dr. Byung-Yoon Ahn (Korea University). The secondary antibodies were α-mouse IgG-HRP and α-rabbit IgG-HRP (Cell Signaling Technology). Proteins were detected using an ECL Kit (ELPIS Biotech, Korea).

Immunoprecipitation

Cells were cotransfected with the indicated plasmids as described in each experiment. Total amounts of DNA were adjusted by adding an empty vector. At the indicated time points after transfection, cells were lysed in buffer containing 25 mM Tris-HCl (pH 7.4), 150 mM sodium chloride (NaCl), 1% NP-40, 1 mM ethylenediaminetetraacetic acid, 5% glycerol, protease inhibitor cocktail, and phosphatase inhibitor cocktail (Thermo Fisher Scientific). Cell lysates were centrifuged at 13,500 rpm at 4°C for 15 min and then supernatant was incubated at 4°C overnight with the indicated antibody. The samples were further incubated with 40 μl of protein A/G beads (Life Technologies, USA) for 1 h. The beads were washed 4 times in washing buffer and then bound protein was detected by immunoblot assay.

Immunofluorescence assay

Huh7 cells grown on cover slides were cotransfected with Myc-tagged NS5A and Flag-tagged IKKε expression plasmid. Cells were washed with PBS and fixed in 4% paraformaldehyde with 0.1% Triton X-100 for 10 min. After three washes with PBS, fixed cells were blocked with 1% bovine serum albumin for 1 h at room temperature. The cells were then incubated with the indicated antibodies overnight at 4°C. After three washes with PBS, cells were incubated with either fluorescein isothiocyanate (FITC)-conjugated α-rabbit IgG or tetramethylrhodamine isothiocyanate (TRITC)-conjugated α-mouse IgG (Cell Signaling Technology) for 1 h at room temperature. After two washes with PBS, cells were counterstained with 4′,6′-diamidino-2-phenylindole (DAPI) to label nuclei. Following three washes with PBS, cells were analyzed using the Zeiss LSM 510 laser confocal microscopy system (Carl Zeiss, Germany).

NanoBRET assay

NanoBRET assay was performed according to the manufacturer's instructions. Briefly, 8×10^5 of Huh7 cells were seeded onto a 6-well plate and incubated for 6 h at 37°C, 5% CO_2. The cells were transfected with indicated concentrations of pHaloTaq-tagged NS5A and pNLF1-tagged IKKε plasmids

(Promega). Each DNA was mixed with Opti-MEM I Reduced Serum Medium, no phenol red (Gibco, USA), and lipofectamine 2000 transfection reagent and incubated for 10 min at room temperature. Cells were transfected with DNA mixture and incubated 20 h at 37°C, 5% CO_2. Cells were washed with Dulbecco's phosphate buffered saline (DPBS), resuspended with trypsin neutralization solution and then centrifuged at 125 × *g* for 5 min. Cells were resuspended in an equal volume of assay medium (Opti-MEM I Reduced Serum Medium, no phenol red + 4% FBS). Approximately 2 × 10^5/ml cells were seeded onto a 96-well plate and incubated for 18 h at 37°C, 5% CO_2. Twenty-five microliters of NanoBRET Nano-Glo substrate (Promega) was added into cells and plate was shaken for 30 s. Mean NanoBRET ratio value was determined by measuring the donor emission (460 nm) and acceptor emission (618 nm).

Statistical analysis

Data are presented as mean ± SD. Statistical analyses were performed by ordinary one-way ANOVA *t*-test using Prism 8 (GraphPad software, USA). The asterisks on the figures indicate significant differences (*$P < 0.05$; **$P < 0.01$; ***$P < 0.001$).

RESULTS

NS5A inhibits IKKε-induced IFN-β production

HCV NS5A protein perturbs host intracellular signaling pathways to regulate host immune responses. To investigate whether NS5A inhibits IFN-β induction, either Huh7 cells or Huh7.5 cells were cotransfected with IFN-β-luc and NS5A expression plasmid and then cells were further infected with SeV, a powerful immune activator. We showed that IFN-β reporter activity was increased by SeV infection (Fig. 1A). However, SeV-induced IFN-β reporter activity was significantly decreased by NS5A at 48 h postinfection in Huh7 cells. Meanwhile, SeV-mediated IFN-β reporter activity was not decreased by NS5A in Huh7.5 cells (Fig. 1B). The sustained virological response rate to IFN therapy varies significantly in HCV patients infected with genotypes 1b and 2a. Notably, NS5A proteins derived from both genotypes 1b and 2a significantly inhibited SeV-induced IFN-β reporter activity. Poly (I:C), a synthetic analog of double-stranded RNA, interacts with TLR3 and acts as a strong IFN inducer by activating the TLR3 signaling pathway. To further investigate whether poly (I:C)-induced IFN-β activity was interrupted by NS5A, HepG2 cells were cotransfected with IFN-β-luc and NS5A expression plasmid, then cells were further transfected with poly I:C. As shown in Fig. 1C, poly (I:C)-induced activation of the IFN-β reporter activity was also significantly inhibited by NS5A.

RNA virus infections are recognized by RIG-I-like receptors, RIG-I, the melanoma differentiation-associated gene (MDA5), and TLR3, which can then induce IFN-β production by activating MAVS, IKKε, and TBK1 (Kawai and Akira, 2006; Saito et al., 2008). To identify the molecules that are affected by NS5A in the IFN signaling pathway, HEK293T cells were transfected with multiple IFN signaling transducers, including RIG-I, MDA5, MAVS, IKKε, and TBK1 in the absence or presence of NS5A. Surprisingly, only IKKε-induced IFN-β promoter induction was significantly inhibited by NS5A in SeV-infected cells (Fig. 1D). TBK1 and IKKε have been previously reported to promote IRF3 and IRF7 phosphorylation and upregulate type I IFNs in the innate immune response (Fitzgerald et al., 2003). To further distinguish between TBK1 and IKKε in the negative role of NS5A in type I IFN signaling pathway, HEK293T cells were cotransfected with IFN-β reporter and TBK1 or IKKε expression plasmid in the absence or presence of NS5A. Cells were then either mock-infected or infected with SeV. We showed that neither TBK1-induced nor IKKε-induced IFN-β reporter activity was altered by NS5A in mock-infected cells (Fig. 1E, left panel). Consistently, both TBK1-and IKKε-induced mRNA, as well as protein levels of IFN-β, were not affected by NS5A in mock-infected cells (Fig. 1E, middle and right panels). Notably, IKKε-induced IFN-β reporter activity was significantly decreased by NS5A in SeV-infected cells, whereas TBK1-induced IFN-β reporter activity was unaffected by NS5A (Fig. 1F, left panel). We confirmed that mRNA and protein levels of IKKε-induced IFN-β were significantly decreased by NS5A in SeV-infected cells (Fig. 1F, middle and right panels). In summary, NS5A specifically inhibits IKKε-induced IFN-β production in SeV-infected cells.

NS5A specifically inhibits IKKε-mediated IFN-β production through DDX3

To investigate the differences in inhibitory activity of IFN-β reporter activity among cell types (Fig. 1), we examined protein expression levels of IFN signal transducers in various cell types. As shown in Fig. 2A, endogenous IKKε and RIG-I expression levels were exceptionally low in both Huh7 and HepG2 cells (lanes 1 and 4), whereas these protein expression levels were relatively high in both Hep3B cells and primary human hepatocytes (lanes 3 and 5). Notably, both IKKε and RIG-I protein levels were barely detected in both Huh7.5 and HEK293T cells (Fig. 2A, lanes 2 and 6). We showed that the endogenous expression level of DDX3 was relatively high in both HepG2 and HEK293T cells (Fig. 2A, lanes 4 and 6).

Overexpression of DDX3 has been previously reported to enhance IFN-β induction through interaction with TBK1/IKKε, whereas silencing of DDX3 suppresses virus-induced IRF3 activation (Gu et al., 2013; Schroder et al., 2008). We therefore hypothesized that HCV NS5A might inhibit IKKε-induced IFN-β induction via DDX3 protein. We demonstrated that IKKε-induced IFN-β reporter activity was increased by DDX3 in a dose-dependent manner (Fig. 2B); as expected, we showed that IKKε- and DDX3-mediated IFN-β reporter activity was decreased by NS5A in a dose-dependent manner (Fig. 2C). Consistently, IKKε- and DDX3-mediated IFN-β mRNA levels were also decreased by NS5A in a dose-dependent manner (Fig. 2D). Importantly, IKKε-induced IFN-β reporter activity was not decreased by NS5A in the absence of DDX3 (Fig. 2E). We therefore investigated whether TBK1- and DDX3-mediated IFN-β promoter activity was also decreased by NS5A. As shown in Fig. 2F, TBK1-induced IFN-β reporter activity was significantly increased by DDX3 (lane 3). Nonetheless, TBK1- and DDX3-mediated IFN-β promoter activity was not altered by NS5A (Fig. 2F, lane 3 vs lanes 4-6). Although IKKε and TBK1 are essential components of the IRF3 signaling pathway, IKKε-mediated, but not TBK1-mediated IFN-β produc-

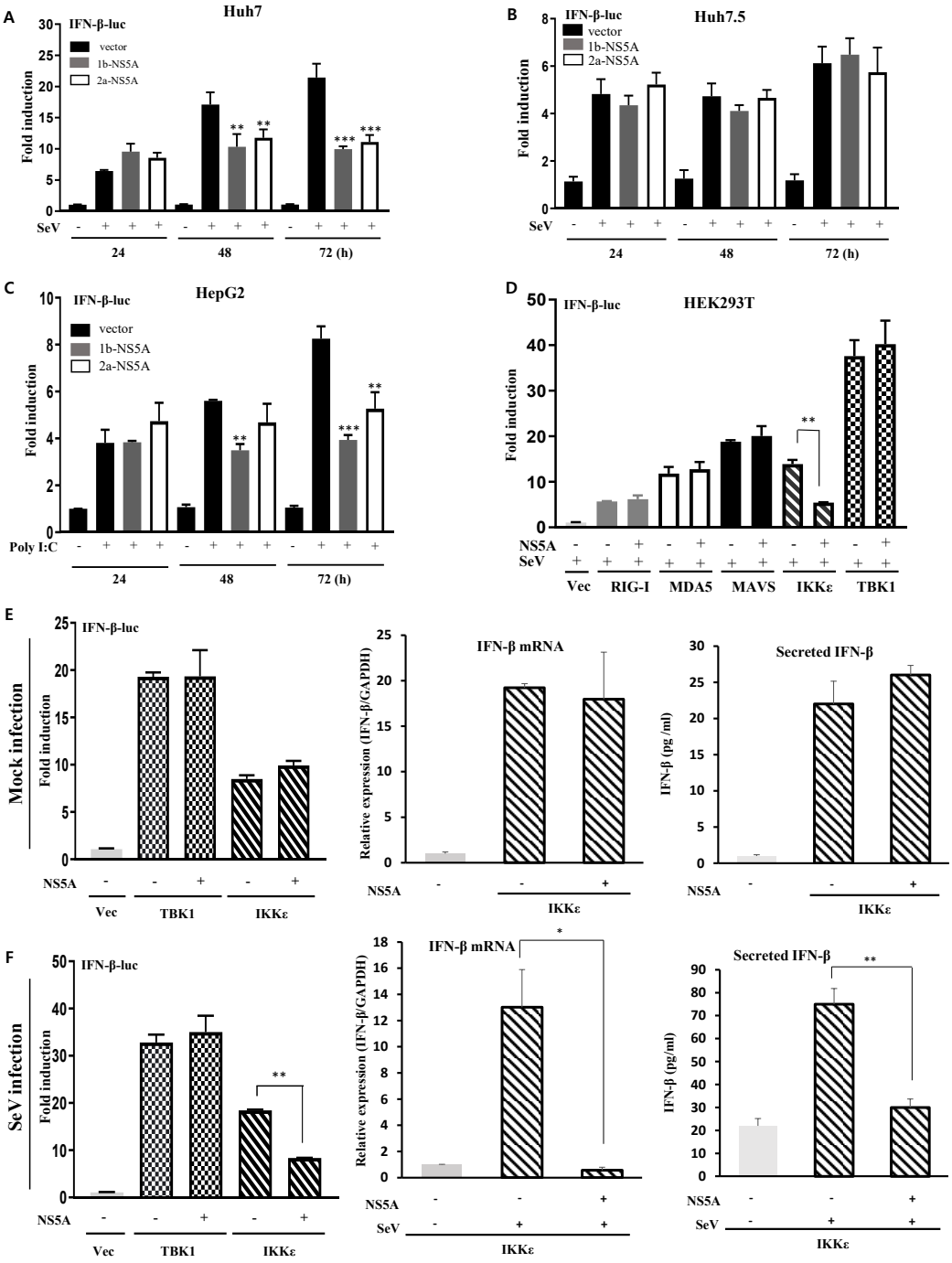

Fig. 1. HCV NS5A inhibits IKKε-induced IFN-β promoter activity. (A and B) Either Huh7 cells (A) or Huh7.5 cells (B) were cotransfected with IFN-β-luc, β-gal, and NS5A expression plasmid. At 12 h after transfection, cells were infected with SeV as described in the Experimental Procedures. IFN-β promoter activity was determined by measuring luciferase activities at the indicated time. (C) HepG2 cells were cotransfected with IFN-β-luc, β-gal, and NS5A expression plasmid. At 12 h after transfection, cells were treated with poly (I:C). IFN-β promoter activity was determined at the indicated time. (D) HEK293T cells were cotransfected with IFN-β reporter plasmid and Flag-tagged RIG, Flag-tagged MDA5, Flag-tagged MAVS, Flag-tagged IKKε, and Flag-tagged TBK1, respectively. At 24 h after transfection, cells were infected with SeV for 18 h, then luciferase activity was measured. (E and F) HEK293T cells were cotransfected with either control vector or IFN-β reporter and Flag-tagged TBK1, IFN-β reporter and Flag-tagged IKKε plasmid as indicated. At 24 h after transfection, cells were either mock-infected (E) or infected with SeV (F). At 18 h postinfection, promoter activities (left panels), mRNA levels (middle panels), and protein levels (right panels) of IFN-β were determined by luciferase reporter assay, qPCR, and ELISA, respectively. The data shown are representative of three independent experiments. $*P < 0.05$; $**P < 0.01$; $***P < 0.001$.

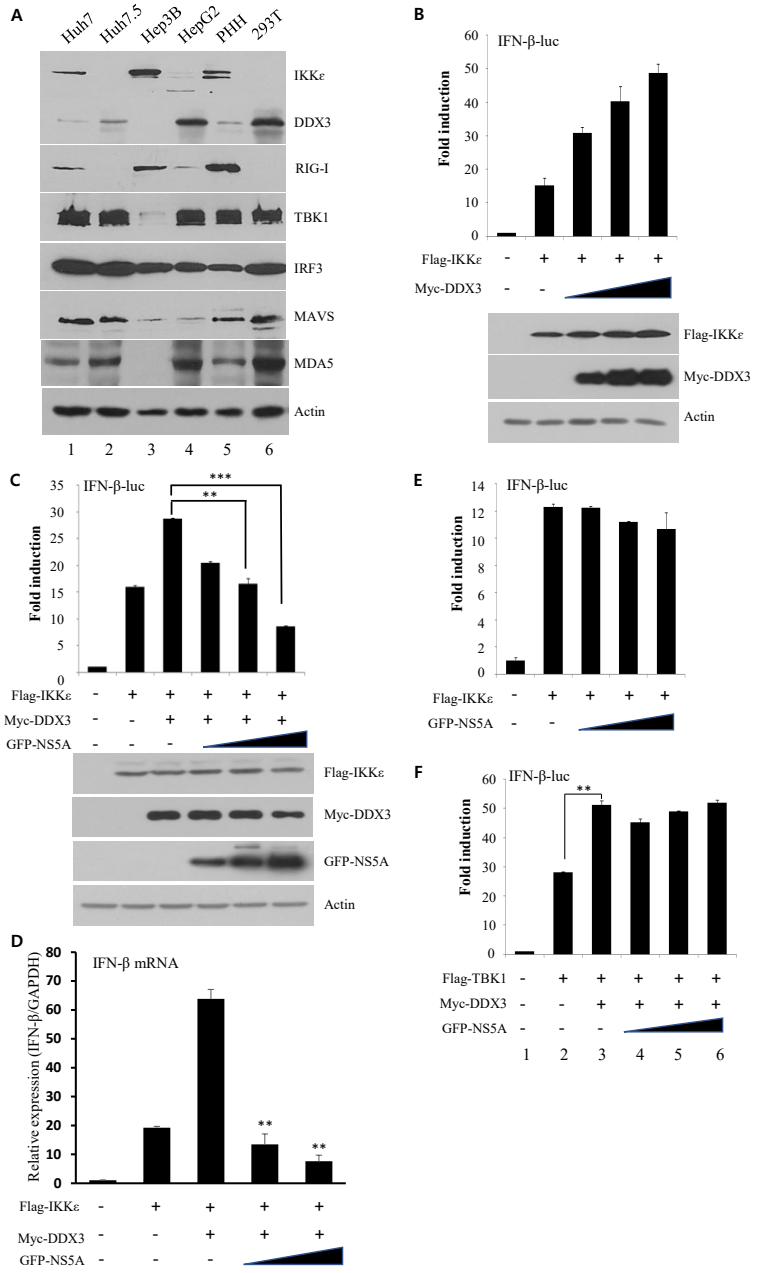

Fig. 2. NS5A inhibits IKK -mediated IFN- promoter activity through DDX3. (A) Endogenous expression levels of viral RNA sensing signaling molecules. Total cell lysates harvested from five different hepatoma cell lines and 293T cells were immunoblotted using the indicated antibodies. (B) (Upper panel) HEK293T cells were cotransfected with the IFN-β reporter and Flag-tagged IKKε plasmid in the absence or presence of various amounts (0.5, 1, and 2 μg) of Myc-tagged DDX3 expression plasmid. At 24 h after transfection, luciferase activity was measured. (Lower panel) Protein expressions were verified by immunoblot analysis using the indicated antibodies. (C) (Upper panel) HEK293T cells were cotransfected with IFN-β reporter plasmid, Flag-tagged IKKε, Myc-tagged DDX3, in the absence or presence of various amounts (0.5, 1, and 2 μg) of GFP-tagged NS5A expression plasmid. At 24 h after transfection, luciferase activity was measured. (Lower panel) Protein expressions were verified by immunoblot analysis using the indicated antibodies. (D) HEK293T cells were cotransfected with IFN-β reporter plasmid, Flag-tagged IKKε, Myc-tagged DDX3 in the presence or absence of various amounts (1 and 2 μg) of GFP-tagged NS5A expression plasmid. At 24 h after transfection, IFN-β mRNA level was determined by qPCR assay. (E) HEK293T cells were cotransfected with IFN-β reporter plasmid and Flag-tagged IKKε in the absence or presence of various amounts (0.5, 1, and 2 μg) of GFP-tagged NS5A expression plasmid. At 24 h after transfection, luciferase activity was determined. (F) HEK293T cells were cotransfected with Flag-tagged TBK1, and Myc-tagged DDX3 in the absence or presence of various amounts of GFP-tagged NS5A expression plasmid. At 24 h after transfection, luciferase activity was measured. The data shown are representative from three independent experiments. All luciferase activities were normalized against β-galactosidase activities. $^{**}P < 0.01$; $^{***}P < 0.001$.

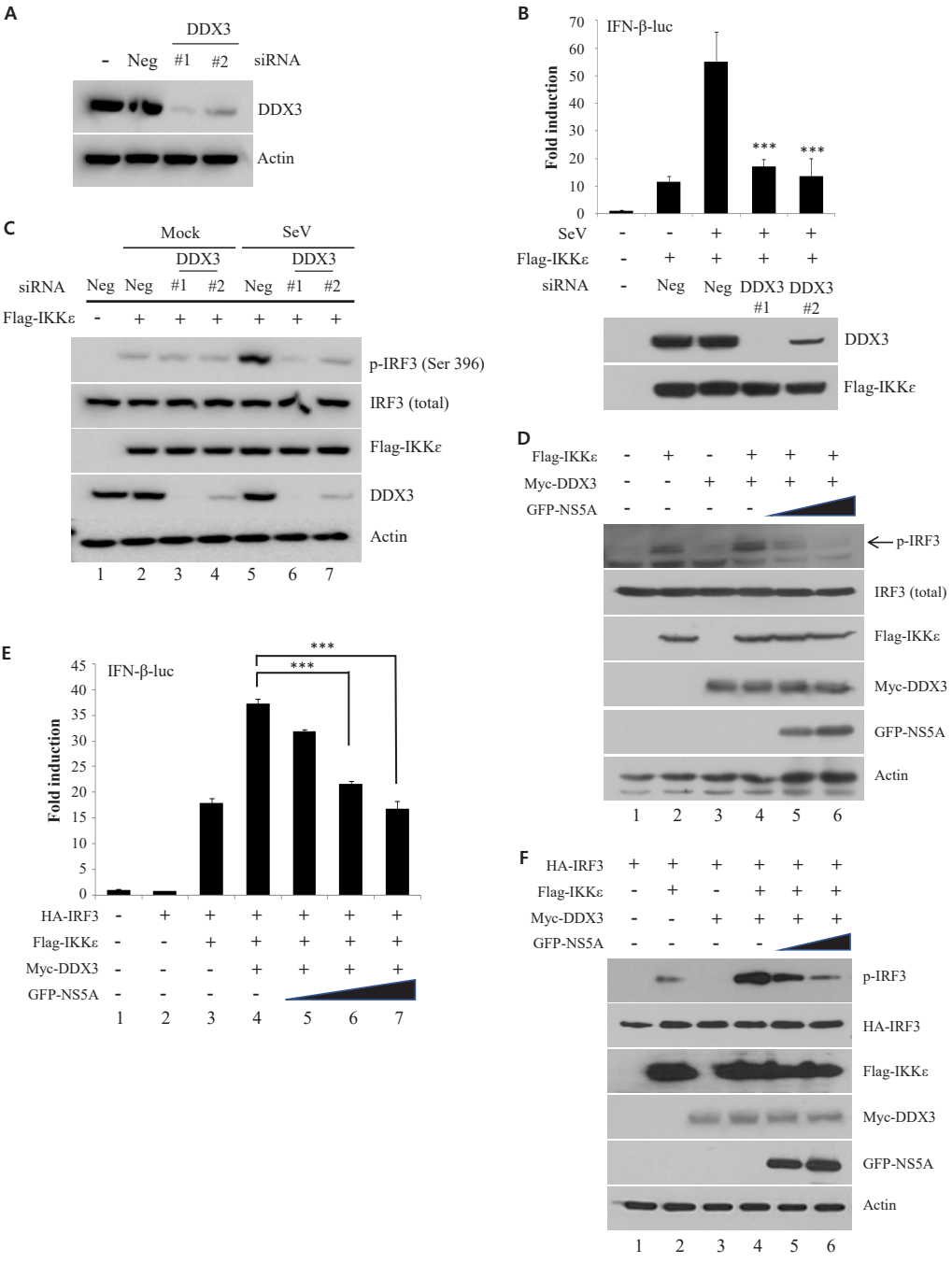

Fig. 3. IKK /DDX3-mediated IRF3 phosphorylation is decreased by NS5A. (A) HEK293T cells were either left untransfected or transfected with negative control siRNA or siRNAs targeting two different regions of DDX3. At 48 h after transfection, protein levels were determined by immunoblot assays using the indicated antibodies. Neg, universal negative-control siRNA. (B) (Upper panel) HEK293T cells were either left untransfected or transfected with negative control siRNA or siRNAs targeting two different regions of DDX3, then further cotransfected with IFN-β reporter plasmid and Flag-tagged IKKε in the absence or presence of 100 HAU/ml of SeV infection. At 18 h postinfection, luciferase activity was measured. (Lower panel) Protein expressions were verified by immunoblot analysis using the indicated antibodies. (C) HEK293T cells were transfected with the indicated siRNAs and Flag-tagged IKKε. At 48 h after transfection, cells were either mock-infected or infected with SeV. At 18 h postinfection, protein expression levels were analyzed by immunoblot assays using the indicated antibodies. (D) HEK293T cells were cotransfected with Flag-tagged-IKKε, Myc-tagged DDX3, and various amounts of GFP-tagged NS5A expression plasmid. At 24 h after transfection, total cell lysates were immunoblotted with the indicated antibodies. (E and F) HEK293T cells were cotransfected with IFN-β reporter plasmid and HA-tagged IRF3, Flag-tagged IKKε, Myc-tagged DDX3, GFP-tagged NS5A plasmid, respectively. At 24 h after transfection, either luciferase activity (E) or protein expression levels (F) were analyzed as described above. $***P < 0.001$.

tion was inhibited by NS5A. These data indicate that NS5A specifically inhibits IKKε-mediated IFN-β production through DDX3.

NS5A inhibits IKKε/DDX3-mediated IRF3 phosphorylation

IRF3 is a major component of the IFN signaling pathway and is activated by IKKε and/or TBK1 (Fitzgerald et al., 2003; Schroder et al., 2008; Tenoever et al., 2007). Silencing of DDX3 has been previously reported to impair IKKε-induced IRF3 phosphorylation at serine 396 (Gu et al., 2013). Since IRF3 is a downstream molecule from IKKε in the IFN-β signaling pathway, we investigated whether IRF3 activity was affected by NS5A. HEK293T cells were transfected with two different siRNAs targeting DDX3, then protein levels were determined. As shown in Fig. 3A, DDX3 protein expression was impaired in DDX3-knockdown cells. Using these siRNAs, we determined the role of DDX3 in IKK -induced IFN-β signaling pathway. We demonstrated that IKK -induced IFN-β promoter activity was significantly increased by SeV infection (Fig. 3B). However, silencing of DDX3 impaired SeV-induced IFN-β promoter activity. We next examined the role of DDX3 in IKK -induced IRF3 activation. HEK293T cells were cotransfected with Flag-tagged IKK and siRNAs targeting DDX3 in the absence or presence of SeV infection. As shown in Fig. 3C, endogenous IRF3 phosphorylation was induced by IKK (lane 2), while IRF3 phosphorylation was not decreased in DDX3-knockdown cells (lanes 3 and 4). Importantly, IKK -induced IRF3 phosphorylation was markedly increased in cells infected with SeV (Fig. 3C, lane 5). Notably, SeV-induced IRF3 phosphorylation was markedly decreased in DDX3-knockdown cells (Fig. 3C, lane 5 vs lanes 6 and 7). These results demonstrated that DDX3 was required for IKK -induced IRF3 phosphorylation in SeV-infected cells.

We then examined whether IKK /DDX3 complex-induced IRF3 phosphorylation was also decreased by NS5A. HEK293T cells were cotransfected with Flag-tagged IKKε and Myc-tagged DDX3 in the absence or presence of various amounts of GFP-tagged NS5A expression plasmid. We showed that endogenous IRF3 phosphorylation was induced by IKKε (Fig. 3D, lane 2) and this was increased by DDX3 (Fig. 3D, lane 4). We further demonstrated that IKKε/DDX3-induced IRF3 phosphorylation was decreased by NS5A in a dose-dependent manner (Fig. 3D, lane 4 vs lanes 5 and 6). To further clarify these results, we overexpressed IRF3, then determined the IKKε/DDX3 complex-induced IFN-β reporter activity. IFN-β promoter activity was not increased by IRF3 expression alone (Fig. 3E, lane 2), whereas this activity was significantly increased by IKKε (Fig. 3E, lane 3). Notably, IKKε-induced IFN-β promoter activity was further increased by DDX3 (Fig. 3E, lane 3 vs lane 4). Using IRF3-overexpressing cells, we conclusively verified that NS5A decreased IKKε/DDX3-mediated IFN-β reporter activity in a dose-dependent manner (Fig. 3E, lanes 5-7). The IRF3 phosphorylation level was consistently increased by IKKε (Fig. 3F, lane 2) and this level was markedly increased by DDX3 in IRF3 overexpressing cells (Fig. 3F, lane 4). Most importantly, the IKKε/DDX3-induced IRF3 phosphorylation level was decreased by NS5A in a dose-dependent manner (Fig. 3F, lanes 5 and 6). These data indicate that NS5A inhibited IKKε/DDX3-mediated IRF3 phosphorylation.

NS5A inhibits DDX3-mediated IKKε phosphorylation

DDX3 directly interacts with IKKε and enhances phosphorylation of IKKε at serine 172 (Gu et al., 2013). To verify this finding, HEK293T cells were cotransfected with Flag-tagged IKKε and Myc-tagged DDX3 expression plasmid; the effect of DDX3 on the phosphorylation of IKKε was determined

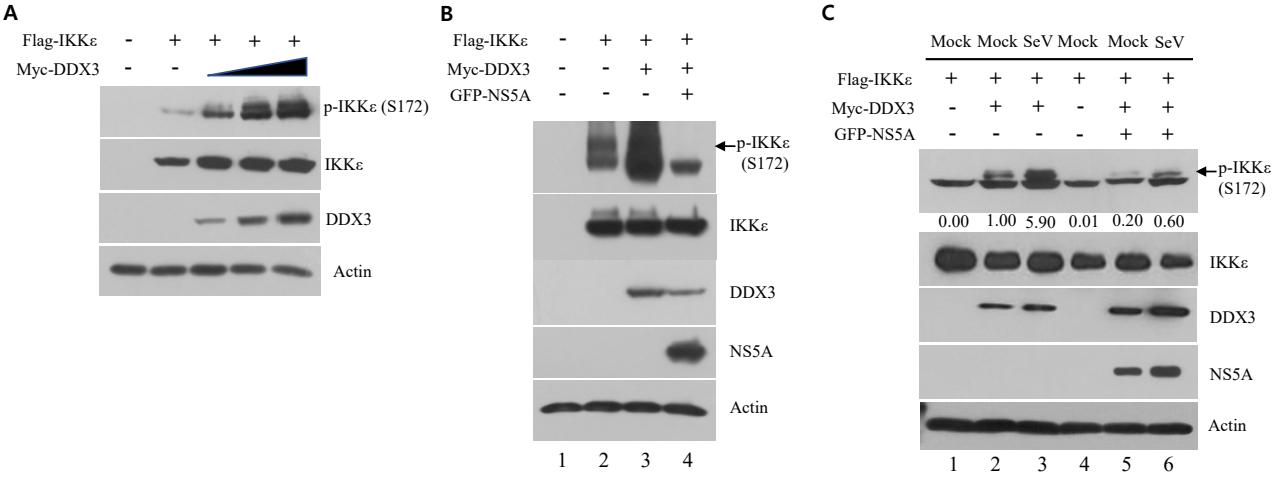

Fig. 4. NS5A inhibits DDX3-mediated IKK phosphorylation. (A) HEK293T cells were cotransfected with Flag-tagged IKKε and various amounts (0.5, 1, and 2 μg) of Myc-tagged DDX3 expression plasmids. At 24 h after transfection, total cell lysates were immunoblotted with the indicated antibodies. (B) HEK293T cells were cotransfected with Flag-tagged IKKε, Myc-tagged DDX3, and GFP-tagged NS5A expression plasmid. At 24 h after transfection, total cell lysates were immunoblotted with the indicated antibodies. (C) HEK293T cells were cotransfected with Flag-tagged IKKε, Myc-tagged DDX3, and GFP-tagged NS5A expression plasmid. At 24 h after transfection, cells were either mock-infected or infected with SeV. At 18 h postinfection, total cell lysates were immunoblotted with the indicated antibodies. Protein band intensity of p-IKKε was determined using ImageJ.

using an anti-S172 antibody. As shown in Fig. 4A, DDX3 increased IKKε phosphorylation at serine 172 in a dose-dependent manner (Fig. 4A). To investigate whether NS5A altered DDX3-induced IKKε phosphorylation, HEK293T cells were cotransfected with Flag-tagged IKKε, Myc-tagged DDX3, and GFP-tagged NS5A plasmid, then total cell lysates were immunoblotted with the indicated antibodies. We showed that the phosphorylation level of IKKε at serine 172 was markedly increased by DDX3 (Fig. 4B, lane 3). Notably, DDX3-induced IKKε phosphorylation was significantly decreased by NS5A (Fig. 4B, lane 4). To further verify this result, we performed the same experiments described in Fig. 4B in both the absence or presence of SeV stimulation. As shown in Fig. 4C, DDX3-induced IKKε phosphorylation was markedly increased by SeV infection (lane 3). Consistently, the DDX3/SeV co-stimulated IKKε phosphorylation level was drastically decreased by NS5A (Fig. 4C, lane 3 vs lane 6). These data clearly show that NS5A modulates the IFN-β signaling pathway by inhibiting DDX3-mediated IKKε phosphorylation.

NS5A interacts with the kinase domain of IKKε

DDX3 interacts with IKKε and enhances IKKε/TBK1-mediated IFN-β promoter induction (Schroder et al., 2008). To investigate whether HCV NS5A interacts with IKKε, HEK293T cells were cotransfected with Flag-tagged IKKε and Myc-tagged NS5A plasmid. We showed that NS5A selectively interacted with IKKε (Fig. 5A, lanes 3 and 6). We further confirmed that NS5A specifically interacted with endogenous IKKε in Huh7 cells (Fig. 5B). We showed that the NS5A protein did not interact with TBK1 (data not shown). These data suggest that NS5A might colocalize with IKKε in cells. To investigate this possibility, Huh7 cells cotransfected with Flag-tagged IKKε and Myc-tagged NS5A expression plasmid were fixed with PFA and an immunofluorescence assay was performed. Results shown in Fig. 5C (left panel) demonstrated that both NS5A and IKKε were widely expressed and colocalized in the cytoplasm as indicated by the yellow fluorescence. We further verified the colocalization of NS5A and IKKε using a NanoBRET assay (Fig. 5C, right). To identify the region in IKKε responsible for NS5A binding, the interaction between NS5A and various deletion mutants of IKKε (Fig. 5D) was determined by a transfection-based coimmunoprecipitation assay. As shown in Fig. 5E, NS5A interacted with the kinase domain (1-299) and with the kinase domain and ubiquitin-like domain (1-383), but not with the coiled-coil domain alone (384-717) or the coiled-coil domain and ubiquitin-like domain (300-717). This result indicated that the kinase domain was responsible for binding with NS5A.

Both the catalytically inactive form of K38A and the auto-phosphorylated inactive form of S172A in the kinase domain have been reported to disrupt IKKε-induced IRF3 phosphorylation and IFN-β induction (Hemalatha et al., 2006). To examine whether these two residues were required for protein interplay with NS5A, we analyzed the binding capabilities of these mutations in IKKε. As shown in Fig. 5F, neither the K38A nor the S172A mutant impaired protein interplay between IKKε and NS5A, indicating that both catalytic and phosphorylation activities of IKKε played no role in protein interaction.

To determine whether the kinase domain of IKKε was required for IFN-β signaling, we determined IFN-β promoter activity using both wild-type and mutant constructs of IKKε. As shown in Fig. 5G, the wild-type but not the kinase domain of IKKε was able to increase IFN-β promoter activity. These data suggest that NS5A may inhibit IFN-β production by disrupting IKKε/DDX3 complex formation. In fact, previous research shows that the C-terminal region of IKKε contains two functional domains, which are both required for the activity of the IFN-β promoter (Nakatsu et al., 2014). Since DDX3 interacts with IKKε and modulates IKKε/TBK1-mediated IFN-β signaling (Schroder et al., 2008), we investigated whether NS5A could alter the protein interplay between IKKε and DDX3. We cotransfected HEK293T cells with Flag-tagged IKKε and Myc-tagged DDX3 in the absence or presence of GFP-tagged NS5A. As shown in Fig. 5H, IKKε interacted with DDX3 (lane 3) and this interaction was disrupted by NS5A in a dose-dependent manner (lanes 4 and 5). These results indicate that NS5A inhibits IKKε-mediated IFN-β signaling by disrupting IKKε and DDX3 interaction.

Hyperphosphorylation of NS5A mediates protein interaction with IKKε and regulates the IFN-β signaling pathway

NS5A is a multifunctional phosphoprotein and exists in two different isoforms, a basal hypophosphorylated (p56) and a hyperphosphorylated (p58) protein (Kaneko et al., 1994; Tanji et al., 1995). A number of serine residues (2194, 2197, 2201, and 2204) in the central region of NS5A are essential for hyperphosphorylation. In addition, hyperphosphorylation of NS5A is involved in HCV RNA replication and protein-protein interaction with viral proteins and cellular proteins (Appel et al., 2005; 2008; Asabe et al., 1997; Masaki et al., 2014; Reed et al., 1997). We therefore tested whether hyperphosphorylation was involved in protein interplay between NS5A and IKKε. Using hyperphosphorylation-defective mutant where the serine residues of 2194, 2197, 2201, and 2204 were substituted with alanine (Fig. 6A, upper), we demonstrated that IKKε interacted with wild-type NS5A but no longer interacted with hyperphosphorylation-defective mutant of NS5A (Fig. 6A, lower panel, lane 2 vs lane 4). We then investigated whether the hyperphosphorylation-defective mutant of NS5A could disrupt IFN-β promoter activity. We showed that wild-type NS5A inhibited IKK /DDX3-mediated IFN-β activity in a dose dependent manner (Fig. 6B, lanes 4 and 5). However, the hyperphosphorylation-defective mutant of NS5A was unable to disrupt IFN-β promoter activity (Fig. 6B, lanes 7 and 8). We further confirmed that protein interplay between IKKε and DDX3 was decreased by wild-type NS5A but not by hyperphosphorylation-defective mutant of NS5A (Fig. 6C, lane 3 vs lane 4). We then investigated the effect of NS5A hyperphosphorylation on IRF3 activation. We showed that DDX3 increased IRF3 the level of phosphorylation, and that this DDX3-potentiated IRF3 phosphorylation level was decreased by wild-type NS5A (Fig. 6D, lane 3 vs lane 4). Notably, the increase in the DDX3-mediated IRF3 phosphorylation level was not altered by the hyperphosphorylation-defective mutant of NS5A (Fig. 6D, lane 3 vs lane 5). These results suggest that hyperphosphorylation of NS5A is required for the protein interaction with IKKε; thus, hyperphosphorylation plays a key

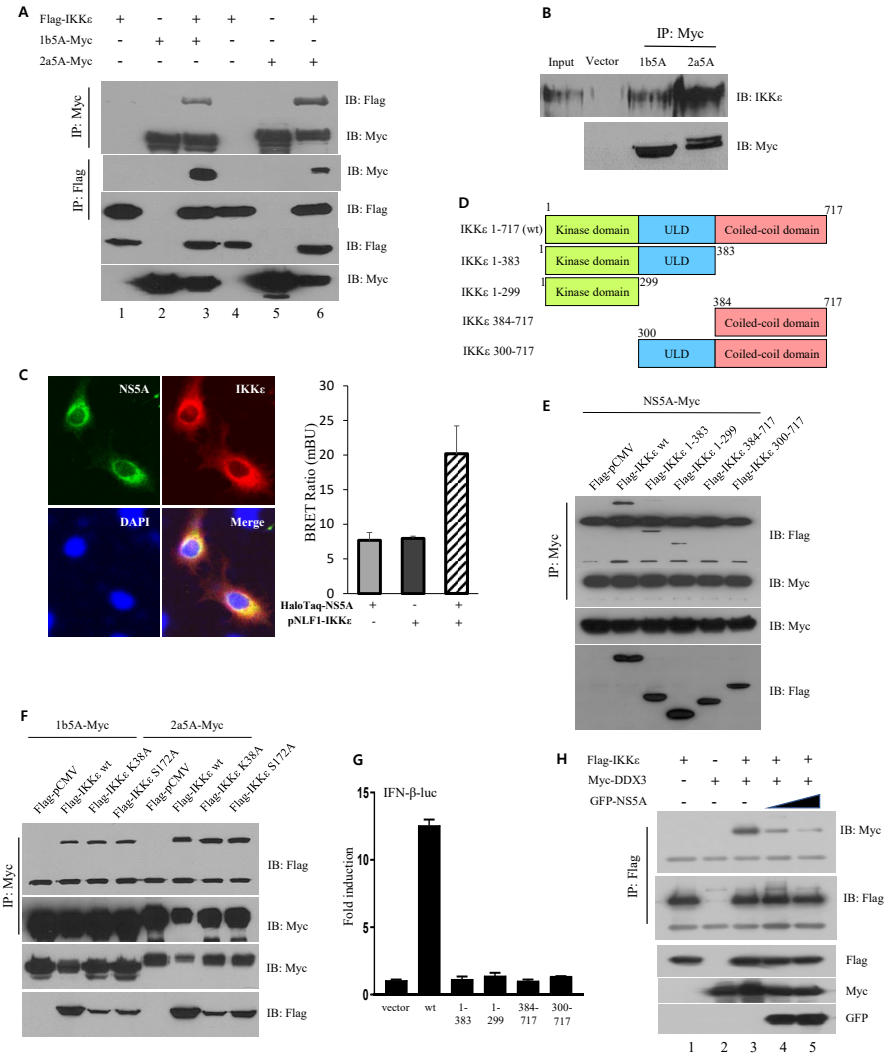

Fig. 5. HCV NS5A interacts with the kinase domain of IKKε. (A) HEK293T cells were cotransfected with Flag-tagged IKKε and Myc-tagged NS5A plasmids. At 36 h after transfection, total cell lysates were immunoprecipitated (IP) and bound proteins were detected by immunoblot (IB) analysis using the indicated antibodies. (B) Huh7 cells were transfected with NS5A plasmid. At 48 h after transfection, total cell lysates were immunoprecipitated with an anti-Myc antibody and the bound protein was detected by immunoblot analysis using an anti-IKKε antibody. (C) (Left) Huh7 cells were cotransfected with Myc-tagged NS5A and Flag-tagged-IKKε expression plasmid. At 48 h after transfection, cells were fixed in 4% PFA (+ 0.1% Triton X-100) and immunofluorescence staining was performed using an anti-Flag monoclonal antibody and TRITC-conjugated goat anti-mouse IgG to detect IKKε (red), and a rabbit anti-Myc antibody and FITC-conjugated goat anti-rabbit IgG to detect NS5A (green). Dual staining showed colocalization of NS5A and IKKε in the cytoplasm as yellow fluorescence in the merged image. Cells were counterstained with DAPI to label nuclei (blue). (Right) Huh7 cells were transfected with either pHaloTaq-tagged NS5A or pNLF1-tagged IKKε plasmid, or cotransfected with pHaloTaq-tagged NS5A and pNLF1-tagged IKKε expression plasmids. At 20 h after transfection, colocalization was determined by NanoBRET assay as described in the Experimental Procedures. (D) A schematic illustration of both wild-type and mutant IKKε. 1-383, Δ coiled-coil domain; 1-299, Δ ubiquitin-like domain (ΔULD) and Δ coiled-coil domain; 384-717, Δ kinase domain and Δ ULD; 300-717, Δ kinase domain. (E) HEK293T cells were cotransfected with Myc-tagged NS5A and Flag-tagged mutants of IKKε expression plasmid. At 48 h after transfection, cell lysates were immunoprecipitated with an anti-Myc antibody, and bound proteins were detected using an anti-Flag antibody. (F) (Top panel) HEK293T cells were cotransfected with Flag-tagged wild-type, mutants of IKKε, and Myc-tagged NS5A plasmid. At 48 h after transfection, total cell lysates were immunoprecipitated with an anti-Myc antibody, then bound proteins were immunoblotted with an anti-Flag antibody to detect wild-type, K38A, and the S172A mutant of IKKε. (Lower three panels) Both immunoprecipitation efficiency and protein expressions were verified using the indicated antibodies. (G) HEK293T cells were cotransfected with IFN-β reporter plasmid and IKKε mutants as indicated. At 24 h after transfection, luciferase activity was measured and normalized against β-galactosidase. (H) (Top panel) HEK293T cells were cotransfected with Flag-tagged IKKε and Myc-tagged DDX3 in the presence or absence of various amounts of GFP-tagged NS5A expression plasmid. At 48 h after transfection, total cell lysates were immunoprecipitated with an anti-Flag antibody, then bound proteins were immunoblotted with an anti-Myc antibody. (Lower three panels) Both immunoprecipitation efficiency and protein expressions were verified by immunoblot analysis using the indicated antibodies.

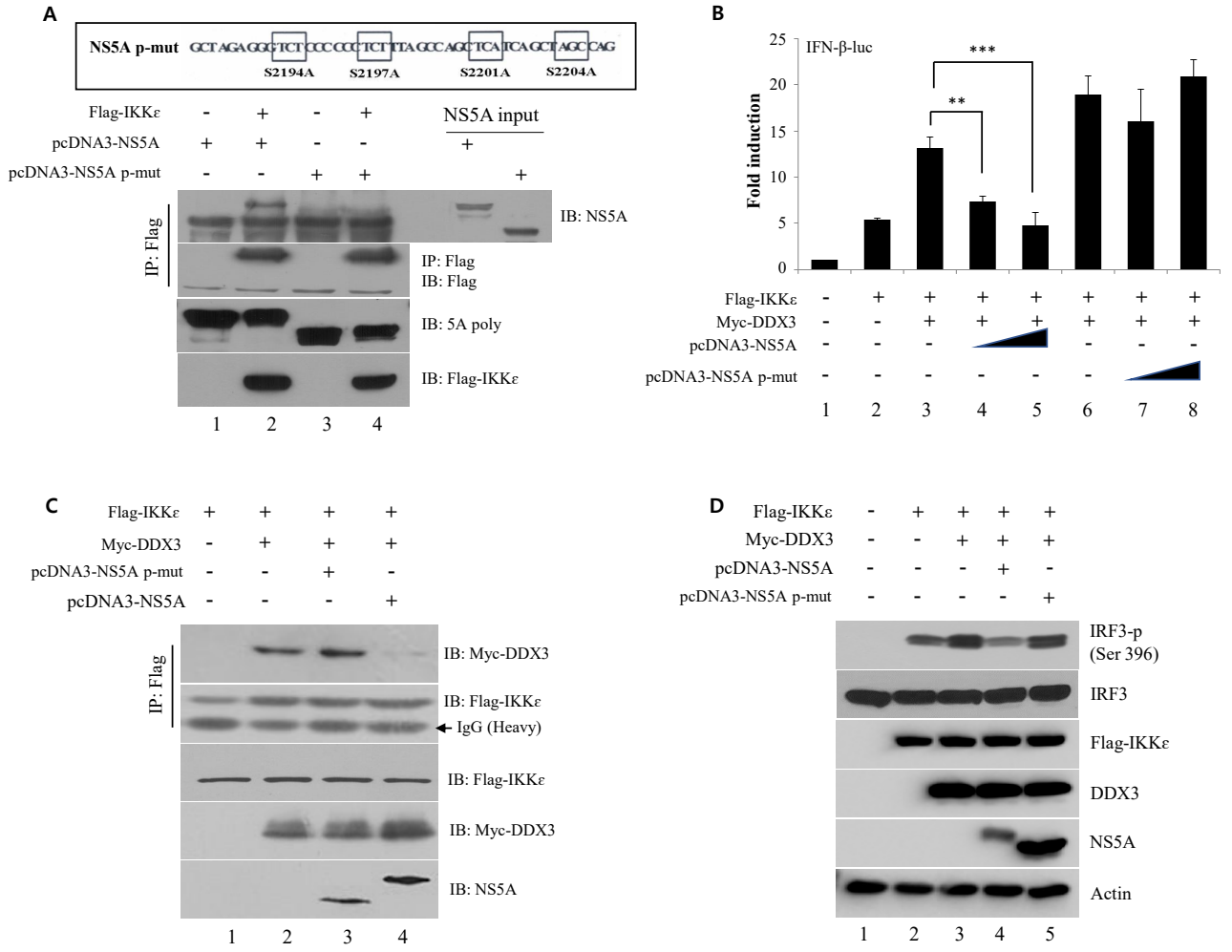

Fig. 6. Hyperphosphorylation of NS5A mediates protein interplay between NS5A and IKKε and is involved in the IFN-β signaling pathway. (A) (Top) A schematic illustration of hyperphosphorylation mutation sites (S2194A, S2197A, S2201A, and S2204A) in NS5A. (Bottom) HEK293T cells were cotransfected with Flag-tagged IKKε and a wild-type or a hyperphosphorylation-defective mutant of NS5A expression plasmid. At 48 h after transfection, total cell lysates were immunoprecipitated with an anti-Flag antibody and bound proteins were immunoblotted with an anti-NS5A antibody. Both immunoprecipitation efficiency and protein expression were verified by immunoblot analysis using the indicated antibodies. (B) HEK293T cells were cotransfected with IFN-β reporter plasmid and Flag-tagged IKKε, Myc-tagged DDX3, pcDNA3-wild-type NS5A, and pcDNA3-hyperphosphorylation-defective mutant of NS5A expression plasmid as indicated. At 24 h after transfection, luciferase activity was measured and normalized against β-galactosidase. (C) HEK293T cells were cotransfected with Flag-tagged IKKε, Myc-tagged DDX3, pcDNA3-wild-type NS5A, and a pcDNA3-hyperphosphorylation-defective mutant of NS5A expression plasmid. At 48 h after transfection, total cell lysates were immunoprecipitated with an anti-Flag antibody and bound proteins were immunoblotted with an anti-Myc antibody. Both immunoprecipitation efficiency and protein expression were detected by immunoblot analysis using the indicated antibodies. (D) HEK293T cells were cotransfected with Flag-tagged IKKε, Myc-tagged DDX3, pcDNA3-wild-type NS5A, and a pcDNA3-hyperphosphorylation-defective mutant of NS5A expression plasmid. At 36 h after transfection, total cell lysates were immunoblotted with the indicated antibodies. $^{**}P < 0.01$; $^{***}P < 0.001$.

role in the inhibitory function of NS5A in the IFN-β signaling pathway.

NS5A inhibits IKKε-induced phosphorylation of NF-κB p65

NF-κB and type I IFN signaling are the major host innate immune responses activated upon viral infection. NF-κB also regulates the expression of many cytokines and immunoregulatory proteins. Since IKKε also modulates NF-κB activity via the regulation of p65 phosphorylation at serine 536 (Adli and Baldwin, 2006), we speculated whether the IKKε/NF-κB signaling pathway was also disturbed by NS5A. We first verified that p65-induced NF-κB activity was significantly increased by IKKε in a dose dependent manner (Fig. 7A, lanes 3-5). We further showed that IKKε-induced NF-κB reporter activity was also inhibited by NS5A in a dose-dependent manner (Fig. 7B, lanes 3 and 4). To determine which signaling transducer-induced NF-κB reporter activity was specifically regulated by NS5A, HEK293T cells were cotransfected with the indi-

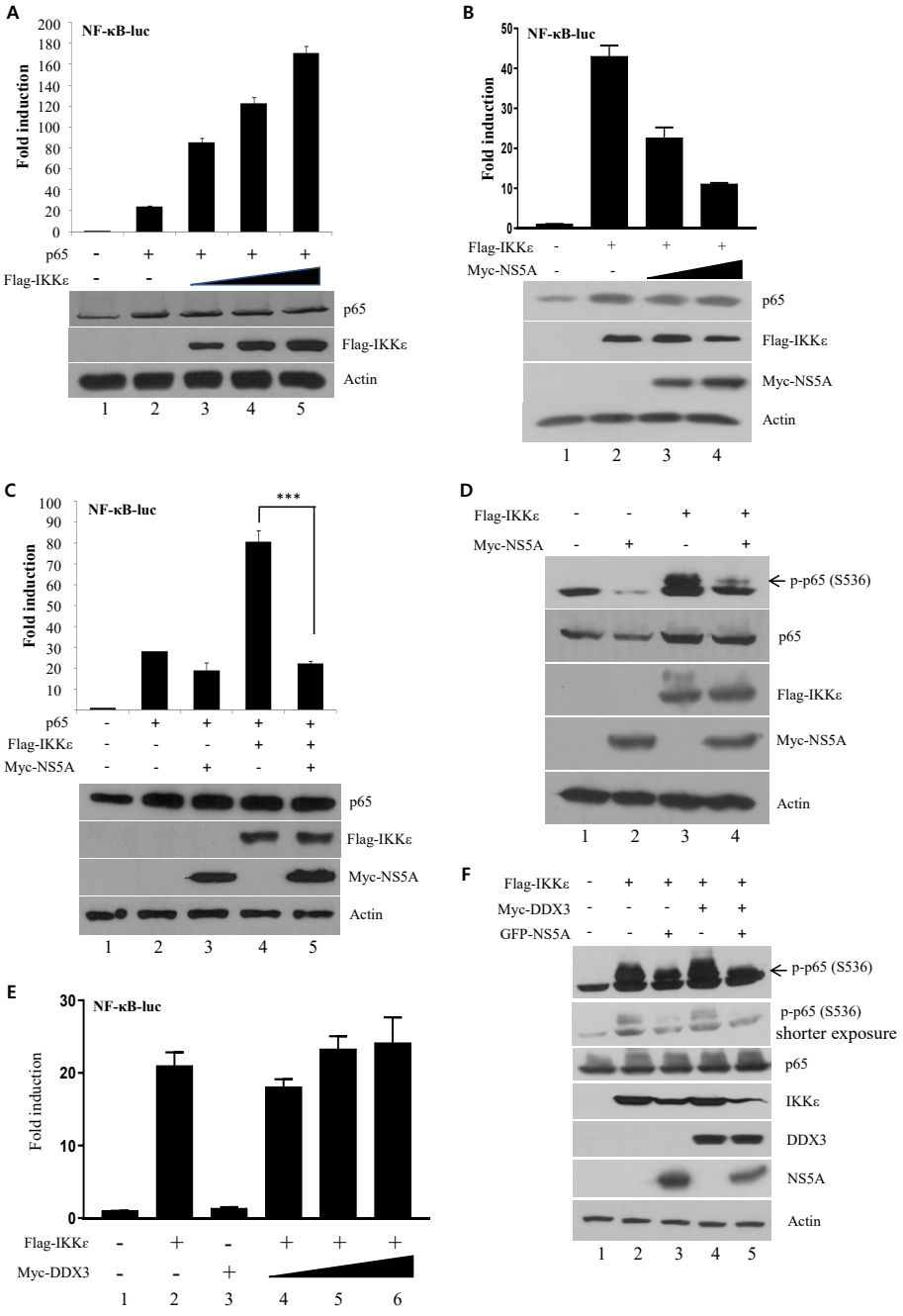

Fig. 7. HCV NS5A inhibits IKKε-induced p65 phosphorylation and NF-κB activation. (A) (Top) HEK293T cells were cotransfected with NF-κB reporter plasmid, pcDNA3.1-p65, and various amounts (0.5, 1, and 1.5 μg) of Flag-tagged IKKε expression plasmid. At 24 h after transfection, luciferase activity was measured. (Bottom) Protein expression was verified by immunoblot analysis using the indicated antibodies. (B) (Top) HEK293T cells were cotransfected with NF-κB reporter plasmid, Flag-tagged IKKε, and increasing amounts of Myc-tagged NS5A expression plasmid. At 24 h after transfection, luciferase activity was determined. (Bottom) Protein expressions were verified by immunoblot analysis using the indicated antibodies. (C) (Top) HEK293T cells were cotransfected with the indicated combinations of plasmid, including NF-κB reporter plasmid, pcDNA3.1-p65, Myc-NS5A, and Flag-tagged-IKKε. At 24 h after transfection, luciferase activity was determined. (Bottom) Protein expression was verified by immunoblot analysis using the indicated antibodies. (D) HEK293T cells were cotransfected with Flag-tagged IKKε and Myc-tagged NS5A expression plasmid. At 24 h after transfection, protein expression levels were determined by immunoblot assay using the indicated antibodies. (E) HEK293T cells were cotransfected with Flag-tagged IKKε and Myc-tagged DDX3 expression plasmid. At 24 h after transfection, luciferase reporter activity was measured and normalized against β-galactosidase. (F) HEK293T cells were cotransfected with Flag-tagged IKKε, Myc-tagged DDX3, and GFP-tagged NS5A expression plasmid. At 24 h after transfection, total cell lysates were subjected to immunoblot analysis using the indicated antibodies. Data are represented as mean ± SD calculated from three independent experiments. $***P < 0.001$.

cated plasmids, then NF-κB reporter activity was determined. As shown in Fig. 7C, p65-induced NF-κB reporter was not altered by NS5A (lane 3). However, IKKε-induced NF-κB reporter was significantly inhibited in cells expressing the NS5A protein (Fig. 7C, lane 5). Because phosphorylation of p65 at serine 536 is important for the activation of NF-κB, we examined whether IKKε-induced p65 phosphorylation was altered by NS5A. Figure 7D shows that IKKε increased the phosphorylation level of p65 (lane 3) and this increase was significantly inhibited by NS5A (lane 3 vs lane 4). This result indicates that NS5A regulates IKKε-mediated p65 phosphorylation.

Next, we explored the possible involvement of DDX3 in IKKε-induced NF-κB reporter activity. As shown in Fig. 7E, NF-κB reporter activity was significantly increased by IKKε. However, IKKε-stimulated NF-κB reporter activity was not altered by DDX3 (Fig. 7E, lanes 4-6). We further examined whether DDX3 was involved in IKKε-induced p65 phosphorylation. Figure 7F demonstrates that IKKε markedly increased the phosphorylation level of P65, but this increase was impaired in cells expressing the NS5A protein (lane 2 vs lane 3). We further showed that the IKKε-induced p65 phosphorylation level was no longer increased by DDX3. These data suggest that NS5A may utilize a different signaling transducer but not DDX3 to inhibit IKKε-induced NF-κB signaling pathway. In summary, HCV regulates not only the type I IFN signaling pathway but also IKKε-mediated NF-κB activity via NS5A to avoid host innate immune response.

DISCUSSION

HCV modulates cellular immune responses to maintain persistent infection in the host. HCV core protein blocks IFN signaling by interacting with the STAT1 SH2 domain and inhibits nuclear import, which in turn inhibits ISG expression (Lin et al., 2006). HCV encodes NS3/4A protease, which blocks RIG-I- and TLR3-induced IFN signaling by cleaving MAVS and TRIF, respectively (Li et al., 2005a; 2005b). The HCV NS5A protein also suppresses the expression of ISGs by disrupting STAT1 phosphorylation and ISGF3 complex formation (Kumthip et al., 2012; Lan et al., 2007). Furthermore, HCV NS5A and E2 inhibit IFN-α-induced antiviral activities by interacting with PKR (Gale et al., 1997; Pavio et al., 2002). NS5A is a multifunctional phosphoprotein consisting of 447 amino acid residues. NS5A exists in two different forms of polypeptide, p56 and p58, which are phosphorylated mainly at serine residues by cellular kinase. We previously demonstrate that NS5A modulated host proteins to promote viral propagation (Choi et al., 2020; Lim et al., 2022) and interferes with various host cell signaling pathways to regulate host immune responses (Choi and Hwang, 2006; Park et al., 2003).

In this study, we investigated the role of NS5A in IFN signaling cascades. We provide several lines of evidence supporting a novel role for HCV NS5A as a negative regulator in the IFN signaling cascade to evade host immune response. First, NS5A inhibits IKKε-induced IFN-β promoter activity. However, TBK1-mediated IFN-β production was not inhibited by NS5A. IKKε and TBK1 are essential components of the IRF3 signaling pathway. TBK1 strongly induces IFN-β activity in the absence of DDX3, while IKKε requires DDX3 to induce IFN-β production. Of note, NS5A interacts with IKKε but not withTBK1. We showed that IKKε-mediated, but not TBK1-mediated IFN-β production was inhibited by NS5A. This is because NS5A specifically inhibits IKKε-mediated IFN-β production through DDX3 by inhibiting DDX3-mediated IKKε phosphorylation. Importantly, IKKε-mediated IFN-β production was inhibited by NS5A if cells were stimulated with SeV infection, suggesting that the IKKε-mediated IFN-β signaling cascade required viral stimulation. Second, NS5A specifically inhibits IKKε-mediated IFN-β production via DDX3. We showed that DDX3 enhanced IKKε-induced IFN-β induction and IRF3 phosphorylation and that this increase was specifically decreased by NS5A in the presence of DDX3. Third, NS5A interacts and colocalizes with IKKε via its kinase domain. Although K38 and S172 play an essential role in antiviral activity, both kinase inactive IKKε (K38A) and phosphorylation-defective IKKε (S172A) mutants are not involved in protein interplay with NS5A. Moreover, the functional domain of IKK alone displayed no IFN-β reporter activity. Indeed, a recent report suggests that the C-terminal 20-aa region (686-705) of IKK is required for IFN-β induction (Nakatsu et al., 2014). NS5A interacts with IKKε via the kinase domain, whereas DDX3 interacts with IKKε via the coiled-coil domain; consistently, NS5A does not share an IKKε binding site with DDX3. We further showed that NS5A does not interact with DDX3 (data not shown). We postulate that an increasing dose of DDX3 may affect protein interaction

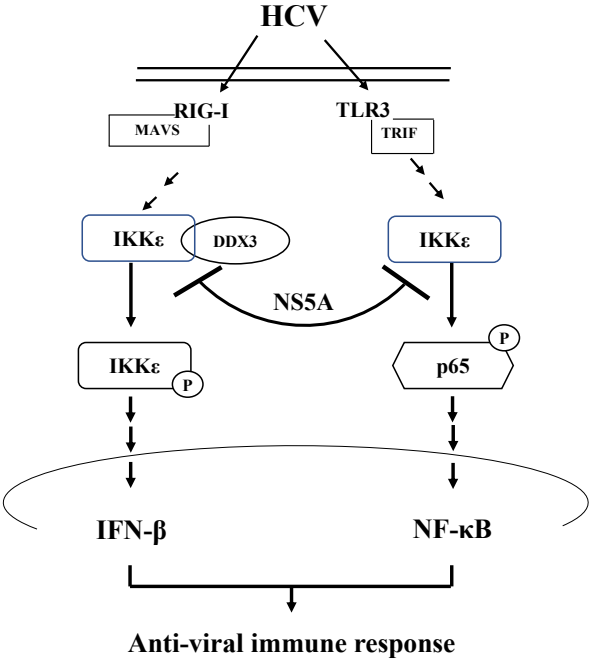

Fig. 8. HCV modulates host innate immune response via the NS5A protein. Type I IFN and NF-κB signaling are the major host innate immune responses activated upon viral infection. HCV modulates host cell immune responses by inhibiting IFN-β production and NF-κB activation via NS5A. HCV NS5A interacts with IKKε and blocks downstream signaling pathways, which can lead to persistent viral infection.

between NS5A and IKKε. Upon HCV infection, host DDX3 protein interacts with IKKε to activate type I IFN production. However, HCV NS5A disrupts the protein interplay between IKKε and DDX3 to evade the host immune response. We speculate that protein interaction between NS5A and IKKε causes a structural change in IKKε, and thus DDX3 is no longer able to interact with IKKε. Whether this region of IKK is involved in negative regulatory function of NS5A in IKK / DDX3-induced antiviral immunity will be investigated in a future study. Fourth, hyperphosphorylation of NS5A is required for the negative regulatory function of NS5A on IKKε-induced antiviral immunity. Hyperphosphorylation of NS5A mediates protein interaction with IKKε and modulates the IFN-β signaling pathway. In fact, a hyperphosphorylation-defective NS5A mutant was unable to inhibit IKKε/DDX3-induced IRF3 phosphorylation and IFN-β promoter activity. Lastly, NS5A inhibits IKKε-induced p65 phosphorylation and NF-κB activation. It has been previously reported that IKKε controls NF-κB activity by regulating phosphorylation of p65 at serine 536 (Adli and Baldwin, 2006). Interestingly, both IKKε-induced p65 phosphorylation and NF-κB activation levels were not altered by DDX3. These data suggest that NS5A may control IKKε-induced antiviral immune response via either a DDX3-dependent or DDX3-independent signaling pathway (Fig. 8).

cGAS recognizes a broad repertoire of cytosolic DNA and activates the endoplasmic reticulum-located adapter STING. Th ecGAS/STING pathway induces both IFN expression and NF-κB-mediated cytokine production. Balka et al. (2020) reported that TBK1 is dispensable for STING-induced NF-κB activation and TBK1 acts redundantly with IKKε to drive NF-kB response upon STING activation. They further reported that activation of IRF3 is highly dependent on TBK1 kinase activity, whereas STING-induced NF-κB activation is less dependent on the kinase activities of TBK1 and IKKε than type I IFNs, i.e., IFN responses are elicited by TBK and IKKε kinase activities. Interestingly, our study showed that IKKε-induced but not TBK1-induced IFN-β reporter activity was significantly decreased by NS5A. Furthermore, both IFNβ and NF-κB activities were downregulated by NS5A. Therefore, it would be of great interest to see the differential effects of NS5A on cGAS/STING-mediated IFNβ/NF-κB responses. Since NS5A interacts with IKKε, and TBK1/IKKε signaling is downstream of cGAS/STING, we questioned whether cGAS/STING-mediated IFN and NF-κB activities were differentially regulated by NS5A. Since we found that neither STING-induced IFNβ activation nor STING-induced NF-κB activation was altered by IKKε (data not shown), we postulate that NS5A may play no role in cGAS/STING signaling. However, further studies are required to determine whether the effects of NS5A on cGAS/STING signaling would display differential effects on IFNβ and NF-κB responses.

The links between dsRNA, IFN induction, NF-κB activation, and PKR are still unclear. PKR is well known for its role in the IFN-induced cellular antiviral response. However, viruses have evolved a mechanism to repress PKR function. HCV NS5A binds PKR to repress kinase function and inhibit PKR-mediated eIF-2α phosphorylation. However, the role of PKR in viral-induced IFNβ production and NF-κB activation remains elusive. To investigate whether the effects of NS5A on IKKε are independent of the effects on PKR, we analyzed IFNβ promoter activity using PKR knock-out Huh7 cells. We found that SeV-induced IFN-β activity was indistinguishably decreased by NS5A in both wild-type and PKR deficient cells (data not shown). These data indicate that the effects of NS5A on IKKε are independent of the effects on PKR.

Upon HCV infection, RIG-I-like receptors sense viral RNAs, where the CARD domain interacts with MAVS, which leads to the activation of type I IFN and NF-κB signaling through activation of IKKε. We showed that DDX3 interacts with IKKε and enhances IRF3 phosphorylation and IFN-β induction. To evade the host response, HCV NS5A interacts with IKKε to disrupt protein interplay between IKKε and DDX3, thereby inhibiting DDX3/IKKε-mediated IFN-β induction. Although the molecular mechanisms of HCV persistence and pathogenesis are not yet fully understood, these processes clearly involve the avoidance of cellular immune responses through the alteration of host signaling pathways. Our findings provide important insights into an additional innate immune evasion mechanism of HCV. We here propose that NS5A is a novel regulator of innate immune signaling pathways, which specifically inhibits IKKε downstream signaling cascades through interaction with IKKε.

ACKNOWLEDGMENTS

We thank Dr. Byeong-Yun Ahn (Korea University, Korea) for Sendai virus and α-NS5A antibody; Dr. S Goodbourn (St George's, University of London, UK) for IFN-β-luc and ISRE-luc plasmids; Dr. Kate Fitzgerald (University of Massachusetts, USA) for Flag-IKK wild-type, K38A, S172A, and TBK1 plasmids; Dr. Andrew G Bowie (Trinity College Dublin, Ireland) for Myc-DDX3 and His-DDX3 plasmids; Dr. Takashi Fujita (Kyoto University, Japan) for pEF-BOS-Flag-RIG-I, Flag-MDA5, MAVS. We also thank Dr. Yun-Sook Lim for critical reading of the manuscript.

This work was supported by grant from the Korea National Institute of Health (2014-NG51001 and 2016-NG51005 for S.M.K.). This work was also supported by the NRF grant funded by the Korea government (MSIT) (2021R1A2C2003275 for S.B.H.).

AUTHOR CONTRIBUTIONS

All authors have given approval to the final version of the manuscript. S.M.K. performed the experiments, analyzed data, and wrote the manuscript. J.Y.P., H.J.H., and B.M.S. performed the experiments. D.T. provided reagents and expertise. B.S.C. provided reagents and supervised the study. S.M.K. and S.B.H. designed experiments and secured funding. S.B.H. supervised the study and wrote the manuscript.

CONFLICT OF INTEREST

The authors have no potential conflicts of interest to disclose.

ORCID

Sang Min Kang https://orcid.org/0000-0002-8189-3028
Ji-Young Park https://orcid.org/0000-0002-9246-6873
Hee-Jeong Han https://orcid.org/0000-0003-3506-3098
Byeong-Min Song https://orcid.org/0000-0003-3370-6512

Dongseob Tark https://orcid.org/0000-0001-7499-4253
Byeong-Sun Choi https://orcid.org/0000-0002-6128-7995
Soon B. Hwang https://orcid.org/0000-0002-8718-1793

REFERENCES

Adli, M. and Baldwin, A.S. (2006). IKK-i/IKKepsilon controls constitutive, cancer cell-associated NF-kappaB activity via regulation of Ser-536 p65/RelA phosphorylation. J. Biol. Chem. *281*, 26976-26984.

Appel, N., Pietschmann, T., and Bartenschlager, R. (2005). Mutational analysis of hepatitis C virus nonstructural protein 5A: potential role of differential phosphorylation in RNA replication and identification of a genetically flexible domain. J. Virol. *79*, 3187-3194.

Appel, N., Zayas, M., Miller, S., Krijnse-Locker, J., Schaller, T., Friebe, P., Kallis, S., Engel, U., and Bartenschlager, R. (2008). Essential role of domain III of nonstructural protein 5A for hepatitis C virus infectious particle assembly. PLoS Pathog. *4*, e1000035.

Asabe, S.I., Tanji, Y., Satoh, S., Kaneko, T., Kimura, K., and Shimotohno, K. (1997). The N-terminal region of hepatitis C virus-encoded NS5A is important for NS4A-dependent phosphorylation. J. Virol. *71*, 790-796.

Balka, K.R., Louis, C., Saunders, T.L., Smith, A.M., Calleja, D.J., D'Silva, D.B., Moghaddas, F., Tailler, M., Lawlor, K.E., Zhan, Y., et al. (2020). TBK1 and IKKε act redundantly to mediate STING-induced NF-κB responses in myeloid cells. Cell Rep. *31*, 107492.

Brownell, J., Bruckner, J., Wagoner, J., Thomas, E., Loo, Y.M., Gale, M., Jr., Liang, T.J., and Polyak, S.J. (2014). Direct, interferon-independent activation of the CXCL10 promoter by NF-kappaB and interferon regulatory factor 3 during hepatitis C virus infection. J. Virol. *88*, 1582-1590.

Choi, J.W., Kim, J.W., Nguyen, L.P., Nguyen, H.C., Park, E.M., Choi, D.H., Han, K.M., Kang, S.M., Tark, D., Lim, Y.S., et al. (2020). Nonstructural NS5A protein regulates LIM and SH3 domain protein 1 to promote hepatitis C virus propagation. Mol. Cells *43*, 469-478.

Choi, S.H. and Hwang, S.B. (2006). Modulation of TGF-beta signal transduction pathway by hepatitis C virus nonstructural 5A protein. J. Biol. Chem. *281*, 7468-7478.

Ferreon, J.C., Ferreon, A.C., Li, K., and Lemon, S.M. (2005). Molecular determinants of TRIF proteolysis mediated by the hepatitis C virus NS3/4A protease. J. Biol. Chem. *280*, 20483-20492.

Fitzgerald, K.A., McWhirter, S.M., Faia, K.L., Rowe, D.C., Latz, E., Golenbock, D.T., Coyle, A.J., Liao, S.M., and Maniatis, T. (2003). IKKepsilon and TBK1 are essential components of the IRF3 signaling pathway. Nat. Immunol. *4*, 491-496.

Gale, M., Jr., Blakely, C.M., Kwieciszewski, B., Tan, S.L., Dossett, M., Tang, N.M., Korth, M.J., Polyak, S.J., Gretch, D.R., and Katze, M.G. (1998). Control of PKR protein kinase by hepatitis C virus nonstructural 5A protein: molecular mechanisms of kinase regulation. Mol. Cell. Biol. *18*, 5208-5218.

Gale, M.J., Jr., Korth, M.J., Tang, N.M., Tan, S.L., Hopkins, D.A., Dever, T.E., Polyak, S.J., Gretch, D.R., and Katze, M.G. (1997). Evidence that hepatitis C virus resistance to interferon is mediated through repression of the PKR protein kinase by the nonstructural 5A protein. Virology *230*, 217-227.

Gu, L., Fullam, A., Brennan, R., and Schroder, M. (2013). Human DEAD box helicase 3 couples IkappaB kinase epsilon to interferon regulatory factor 3 activation. Mol. Cell. Biol. *33*, 2004-2015.

Hoofnagle, J.H. (2002). Course and outcome of hepatitis C. Hepatology *36*(5 Suppl 1), S21-S29.

Indukuri, H., Castro, S.M., Liao, S.M., Feeney, L.A., Dorsch, M., Coyle, A.J., Garofalo, R.P., Brasier, A.R., and Casola, A. (2006). Ikkepsilon regulates viral-induced interferon regulatory factor-3 activation via a redox-sensitive pathway. Virology *353*, 155-165.

Jensen, S. and Thomsen, A.R. (2012). Sensing of RNA viruses: a review of innate immune receptors involved in recognizing RNA virus invasion. J. Virol. *86*, 2900-2910.

Kanda, T., Steele, R., Ray, R., and Ray, R.B. (2007). Hepatitis C virus infection induces the beta interferon signaling pathway in immortalized human hepatocytes. J. Virol. *81*, 12375-12381.

Kaneko, T., Tanji, Y., Satoh, S., Hijikata, M., Asabe, S., Kimura, K., and Shimotohno, K. (1994). Production of two phosphoproteins from the NS5A region of the hepatitis C viral genome. Biochem. Biophys. Res. Commun. *205*, 320-326.

Kawai, T. and Akira, S. (2006). Innate immune recognition of viral infection. Nat. Immunol. *7*, 131-137.

Kawai, T. and Akira, S. (2008). Toll-like receptor and RIG-I-like receptor signaling. Ann. N. Y. Acad. Sci. *1143*, 1-20.

Kawai, T., Takahashi, K., Sato, S., Coban, C., Kumar, H., Kato, H., Ishii, K.J., Takeuchi, O., and Akira, S. (2005). IPS-1, an adaptor triggering RIG-I- and Mda5-mediated type I interferon induction. Nat. Immunol. *6*, 981-988.

Kumthip, K., Chusri, P., Jilg, N., Zhao, L., Fusco, D.N., Zhao, H., Goto, K., Cheng, D., Schaefer, E.A., Zhang, L., et al. (2012). Hepatitis C virus NS5A disrupts STAT1 phosphorylation and suppresses type I interferon signaling. J. Virol. *86*, 8581-8591.

Lan, K.H., Lan, K.L., Lee, W.P., Sheu, M.L., Chen, M.Y., Lee, Y.L., Yen, S.H., Chang, F.Y., and Lee, S.D. (2007). HCV NS5A inhibits interferon-alpha signaling through suppression of STAT1 phosphorylation in hepatocyte-derived cell lines. J. Hepatol. *46*, 759-767.

Lau, D.T., Fish, P.M., Sinha, M., Owen, D.M., Lemon, S.M., and Gale, M., Jr. (2008). Interferon regulatory factor-3 activation, hepatic interferon-stimulated gene expression, and immune cell infiltration in hepatitis C virus patients. Hepatology *47*, 799-809.

Li, K., Foy, E., Ferreon, J.C., Nakamura, M., Ferreon, A.C., Ikeda, M., Ray, S.C., Gale, M., Jr., and Lemon, S.M. (2005a). Immune evasion by hepatitis C virus NS3/4A protease-mediated cleavage of the Toll-like receptor 3 adaptor protein TRIF. Proc. Natl. Acad. Sci. U. S. A. *102*, 2992-2997.

Li, Q., Brass, A.L., Ng, A., Hu, Z., Xavier, R.J., Liang, T.J., and Elledge, S.J. (2009). A genome-wide genetic screen for host factors required for hepatitis C virus propagation. Proc. Natl. Acad. Sci. U. S. A. *106*, 16410-16415.

Li, S., Wang, L., Berman, M., Kong, Y.Y., and Dorf, M.E. (2011). Mapping a dynamic innate immunity protein interaction network regulating type I interferon production. Immunity *35*, 426-440.

Li, X.D., Sun, L., Seth, R.B., Pineda, G., and Chen, Z.J. (2005b). Hepatitis C virus protease NS3/4A cleaves mitochondrial antiviral signaling protein off the mitochondria to evade innate immunity. Proc. Natl. Acad. Sci. U. S. A. *102*, 17717-17722.

Lim, Y.S., Nguyen, M.T.N., Pham, T.X., Huynh, T.T.X., Park, E.M., Choi, D.H., Kang, S.M., Tark, D., and Hwang, S.B. (2022). Hepatitis C virus NS5A protein interacts with telomere length regulation protein: implications for telomere shortening in patients infected with HCV. Mol. Cells *45*, 148-157.

Lin, R., Heylbroeck, C., Pitha, P.M., and Hiscott, J. (1998). Virus-dependent phosphorylation of the IRF-3 transcription factor regulates nuclear translocation, transactivation potential, and proteasome-mediated degradation. Mol. Cell. Biol. *18*, 2986-2996.

Lin, W., Kim, S.S., Yeung, E., Kamegaya, Y., Blackard, J.T., Kim, K.A., Holtzman, M.J., and Chung, R.T. (2006). Hepatitis C virus core protein blocks interferon signaling by interaction with the STAT1 SH2 domain. J. Virol. *80*, 9226-9235.

Lindenbach, B.D. and Rice, C.M. (2005). Unravelling hepatitis C virus replication from genome to function. Nature *436*, 933-938.

Masaki, T., Matsunaga, S., Takahashi, H., Nakashima, K., Kimura, Y., Ito, M., Matsuda, M., Murayama, A., Kato, T., Hirano, H., et al. (2014). Involvement of hepatitis C virus NS5A hyperphosphorylation mediated by casein kinase I-alpha in infectious virus production. J. Virol. *88*, 7541-7555.

Matsumoto, M., Hwang, S.B., Jeng, K.S., Zhu, N., and Lai, M.M. (1996).

Homotypic interaction and multimerization of hepatitis C virus core protein. Virology *218*, 43-51.

Metz, P., Reuter, A., Bender, S., and Bartenschlager, R. (2013). Interferon-stimulated genes and their role in controlling hepatitis C virus. J. Hepatol. *59*, 1331-1341.

Morikawa, K., Lange, C.M., Gouttenoire, J., Meylan, E., Brass, V., Penin, F., and Moradpour, D. (2011). Nonstructural protein 3-4A: the Swiss army knife of hepatitis C virus. J. Viral Hepat. *18*, 305-315.

Nakatsu, Y., Matsuoka, M., Chang, T.H., Otsuki, N., Noda, M., Kimura, H., Sakai, K., Kato, H., Takeda, M., and Kubota, T. (2014). Functionally distinct effects of the C-terminal regions of IKKepsilon and TBK1 on type I IFN production. PLoS One *9*, e94999.

Ng, S.L., Friedman, B.A., Schmid, S., Gertz, J., Myers, R.M., Tenoever, B.R., and Maniatis, T. (2011). IkappaB kinase epsilon (IKK(epsilon)) regulates the balance between type I and type II interferon responses. Proc. Natl. Acad. Sci. U. S. A. *108*, 21170-21175.

Nguyen, L.P., Nguyen, T.T.T., Nguyen, H.C., Pham, H.T., Han, K.M., Choi, D.H., Park, E.M., Kang, S.M., Tark, D., Lim, Y.S., et al. (2020). Cortactin interacts with hepatitis C virus core and NS5A proteins: implications for virion assembly. J. Virol. *94*, e01306-20.

Noguchi, T., Satoh, S., Noshi, T., Hatada, E., Fukuda, R., Kawai, A., Ikeda, S., Hijikata, M., and Shimotohno, K. (2001). Effects of mutation in hepatitis C virus nonstructural protein 5A on interferon resistance mediated by inhibition of PKR kinase activity in mammalian cells. Microbiol. Immunol. *45*, 829-840.

Oshiumi, H., Sakai, K., Matsumoto, M., and Seya, T. (2010). DEAD/H BOX 3 (DDX3) helicase binds the RIG-I adaptor IPS-1 to up-regulate IFN-beta-inducing potential. Eur. J. Immunol. *40*, 940-948.

Park, K.J., Choi, S.H., Choi, D.H., Park, J.M., Yie, S.W., Lee, S.Y., and Hwang, S.B. (2003). Hepatitis C virus NS5A protein modulates c-Jun N-terminal kinase through interaction with tumor necrosis factor receptor-associated factor 2. J. Biol. Chem. *278*, 30711-30718.

Pavio, N., Taylor, D.R., and Lai, M.M. (2002). Detection of a novel unglycosylated form of hepatitis C virus E2 envelope protein that is located in the cytosol and interacts with PKR. J. Virol. *76*, 1265-1272.

Perwitasari, O., Cho, H., Diamond, M.S., and Gale, M., Jr. (2011). Inhibitor of kappaB kinase epsilon (IKK(epsilon)), STAT1, and IFIT2 proteins define novel innate immune effector pathway against West Nile virus infection. J. Biol. Chem. *286*, 44412-44423.

Polyak, S.J., Khabar, K.S., Paschal, D.M., Ezelle, H.J., Duverlie, G., Barber, G.N., Levy, D.E., Mukaida, N., and Gretch, D.R. (2001). Hepatitis C virus nonstructural 5A protein induces interleukin-8, leading to partial inhibition of the interferon-induced antiviral response. J. Virol. *75*, 6095-6106.

Ray, R.B. and Ray, R. (2001). Hepatitis C virus core protein: intriguing properties and functional relevance. FEMS Microbiol. Lett. *202*, 149-156.

Reed, K.E. and Rice, C.M. (2000). Overview of hepatitis C virus genome structure, polyprotein processing, and protein properties. Curr. Top. Microbiol. Immunol. *242*, 55-84.

Reed, K.E., Xu, J., and Rice, C.M. (1997). Phosphorylation of the hepatitis C virus NS5A protein in vitro and in vivo: properties of the NS5A-associated kinase. J. Virol. *71*, 7187-7197.

Reyes, G.R. (2002). The nonstructural NS5A protein of hepatitis C virus: an expanding, multifunctional role in enhancing hepatitis C virus pathogenesis. J. Biomed. Sci. *9*, 187-197.

Saito, I., Miyamura, T., Ohbayashi, A., Harada, H., Katayama, T., Kikuchi, S., Watanabe, Y., Koi, S., Onji, M., and Ohta, Y. (1990). Hepatitis C virus infection is associated with the development of hepatocellular carcinoma. Proc. Natl. Acad. Sci. U. S. A. *87*, 6547-6549.

Saito, T., Owen, D.M., Jiang, F., Marcotrigiano, J., and Gale, M., Jr. (2008). Innate immunity induced by composition-dependent RIG-I recognition of hepatitis C virus RNA. Nature *454*, 523-527.

Schroder, M., Baran, M., and Bowie, A.G. (2008). Viral targeting of DEAD box protein 3 reveals its role in TBK1/IKKepsilon-mediated IRF activation. EMBO J. *27*, 2147-2157.

Seth, R.B., Sun, L., Ea, C.K., and Chen, Z.J. (2005). Identification and characterization of MAVS, a mitochondrial antiviral signaling protein that activates NF-kappaB and IRF 3. Cell *122*, 669-682.

Sharma, S., tenOever, B.R., Grandvaux, N., Zhou, G.P., Lin, R., and Hiscott, J. (2003). Triggering the interferon antiviral response through an IKK-related pathway. Science *300*, 1148-1151.

Tanji, Y., Kaneko, T., Satoh, S., and Shimotohno, K. (1995). Phosphorylation of hepatitis C virus-encoded nonstructural protein NS5A. J. Virol. *69*, 3980-3986.

Tenoever, B.R., Ng, S.L., Chua, M.A., McWhirter, S.M., Garcia-Sastre, A., and Maniatis, T. (2007). Multiple functions of the IKK-related kinase IKKepsilon in interferon-mediated antiviral immunity. Science *315*, 1274-1278.

Wong, A.H., Tam, N.W., Yang, Y.L., Cuddihy, A.R., Li, S., Kirchhoff, S., Hauser, H., Decker, T., and Koromilas, A.E. (1997). Physical association between STAT1 and the interferon-inducible protein kinase PKR and implications for interferon and double-stranded RNA signaling pathways. EMBO J. *16*, 1291-1304.

Yu, M. and Levine, S.J. (2011). Toll-like receptor, RIG-I-like receptors and the NLRP3 inflammasome: key modulators of innate immune responses to double-stranded RNA viruses. Cytokine Growth Factor Rev. *22*, 63-72.

Yu, S., Chen, J., Wu, M., Chen, H., Kato, N., and Yuan, Z. (2010). Hepatitis B virus polymerase inhibits RIG-I- and Toll-like receptor 3-mediated beta interferon induction in human hepatocytes through interference with interferon regulatory factor 3 activation and dampening of the interaction between TBK1/IKKepsilon and DDX3. J. Gen. Virol. *91*, 2080-2090.